

## Supplementary information

to

### Epitaxial growth of perovskite oxide films facilitated by oxygen vacancies

M. Tyunina<sup>1,2</sup>, L. L. Rusevich<sup>3</sup>, E. A. Kotomin<sup>3,4</sup>, O. Pacherova<sup>2</sup>, T. Kocourek<sup>2</sup>, A. Dejneka<sup>2</sup>

<sup>1</sup>Microelectronics Research Unit, Faculty of Information Technology and Electrical Engineering, University of Oulu, P. O. Box 4500, FI-90014 Oulu, Finland

<sup>2</sup>Institute of Physics of the Czech Academy of Sciences, Na Slovance 2, 18221 Prague, Czech Republic

<sup>3</sup>Institute of Solid State Physics, University of Latvia, Kengaraga Str. 8, LV-1063 Riga, Latvia

<sup>4</sup>Max Planck Institute for Solid State Research, Heisenberg Str. 1, Stuttgart D-70569, Germany

#### **S1. Epitaxy and elastic relationships.**

**Fig. S1.** Schematics of cube-on-cube epitaxy.

#### **S2. Pulsed laser deposition.**

**Fig. S2.** Growth kinetics in pulsed laser deposition of STO.

#### **S3. Crystal structure.**

**Fig. S3.** XRD  $\Theta$ - $2\Theta$  scans.

**Fig. S4.** Reciprocal space maps around (002) lattice points.

**Fig. S5.** Details of XRD  $\Theta$ - $2\Theta$  scans around (001) perovskite peaks.

**Fig. S6.** XRD  $\Theta$ - $2\Theta$  scans around (002) perovskite peaks in the strained and relaxed films.

#### **S4. Optical losses.**

**Fig. S7.** Extinction coefficient as a function of wavelength.

#### **S5. Anisotropic chemical expansion.**

#### **S6. Tetragonal material.**

**Fig. S8.** Lattice parameters of tetragonal material.

#### **S7. First-principles analysis of elastic properties.**

#### **S8. Interaction of oxygen vacancy stresses with misfit strain.**

#### **S9. Residual strain.**

**Fig. S9.** Out-of-plane strain in the films.

### S1. Epitaxy and elastic relationships.

During epitaxial growth, a thin film of a material is formed on the top of a substrate, whose crystal symmetry and lattice parameters may differ from those of the material. Here, a cube-on-cube epitaxy of a cubic material (lattice parameter  $a_0$ ) on a cubic substrate (lattice parameter  $a_{SUB}$ ) is considered [Fig. S1(a)]. This case is valid for STO on LSAT. Because of the material-substrate mismatch in lattice parameters, the substrate imposes biaxial in-plane compressive stress on the material, whereas there is no out-of-plane stress [Fig. S1(b)]. For a coherent film, where the in-plane lattice parameters  $a$  equals to those of the underlying substrate, the substrate-imposed stress leads to a new out-of-plane lattice parameter  $c$ , which differs from  $a_0$  in the material [Fig. S1(c)]. The lattice parameters, tetragonality, and unit-cell volume in the mechanically stressed (strained) film differ from those in the material and can be estimated as follows.

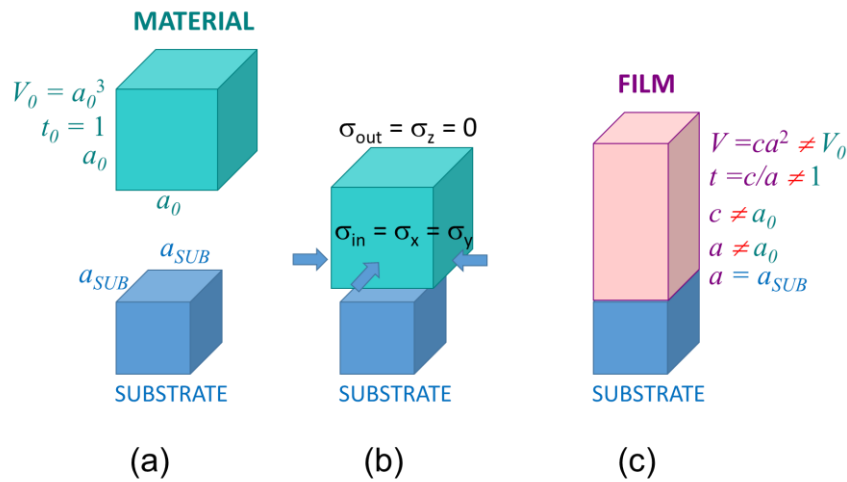


**Fig. S1.** Schematics of cube-on-cube epitaxy. (a) Unit cells of the material and substrate. (b) Substrate-imposed mechanical conditions. (c) Unit cell of the strained film.

The theoretical material-substrate misfit strain is

$$s_a = \frac{a_{SUB}}{a_0} - 1. \quad (1)$$

This strain is compressive, approximately -0.95 % for STO/LSAT:  $a_{SUB} = 3.868 \text{ \AA}$  and  $a_0 = 3.905 \text{ \AA}$  are the lattice parameters of LSAT and STO, respectively.

For the coherent strained cube-on-cube film [Fig. 1(c)], the in-plane lattice parameters are similar and equal to

$$a = b = a_{SUB} \quad (2)$$

The out-of-plane strain ( $s_c$ ) and the out-of-plane lattice parameter ( $c$ ) are elastically related to the in-plane strain ( $s_a$ ):

$$s_c = -\frac{2c_{12}}{c_{11}} s_a \quad (3)$$

$$c = a_0(1 + s_c) = a_0 \left(1 - \frac{2c_{12}}{c_{11}} s_a\right) \quad (4)$$

The elastic constants of STO are  $c_{11} = 3.48 \times 10^{11}$  N/m<sup>2</sup> and  $c_{12} = 1.03 \times 10^{11}$  N/m<sup>2</sup>.

The unit-cell volume  $V$  and tetragonality  $t$  of the strained film are, correspondingly:

$$V = ca^2 = a_0^3(1 + s_a)^2 \left(1 - \frac{2c_{12}}{c_{11}} s_a\right) \quad (5)$$

$$t = \frac{c}{a} = \frac{\left(1 - \frac{2c_{12}}{c_{11}} s_a\right)}{(1 + s_a)} \quad (6)$$

The relationships (3-6) make it possible not only to calculate theoretical lattice parameters of the strained film, but also to perform reverse estimations. They allow for determining the lattice parameter  $a_0$  of an unknown cubic material using the lattice parameters  $a$  and  $c$ , which are experimentally measured in the film made of such material. The strain  $s_a$  can be found from (6) and then the parameter  $a_0$  can be calculated using (4) or (5).

## S2. Pulsed laser deposition.

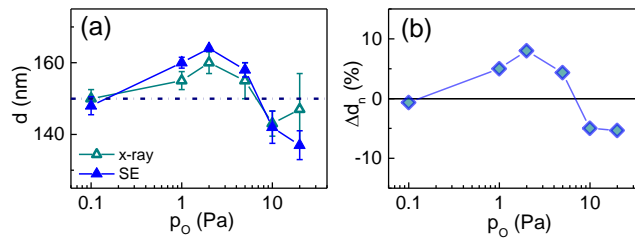


**Fig. S2.** Growth kinetics in pulsed laser deposition of STO. (a) Thickness and (b) thickness variation as a function of oxygen pressure. Data were obtained by x-ray reflectivity and/or by x-ray diffraction (from Laue satellites) and by spectroscopic ellipsometry (a). Data are averaged in (b).

### S3. Crystal structure.

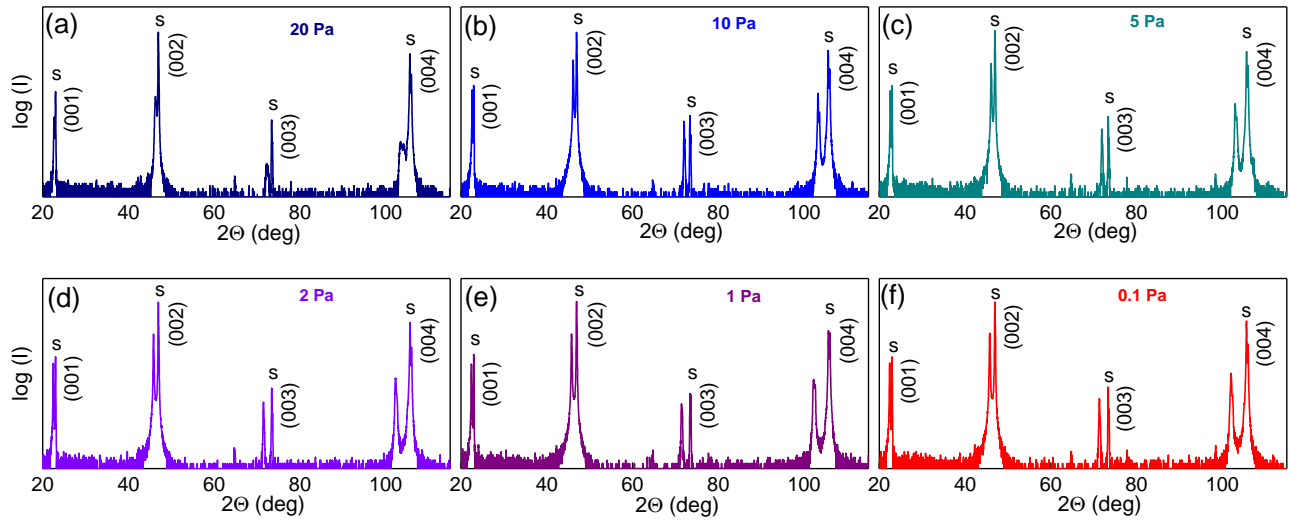


**Fig. S3.** XRD  $\Theta$ - $2\Theta$  scans in the 150-nm-thick STO films on LSAT. Deposition pressure is marked on the plots.

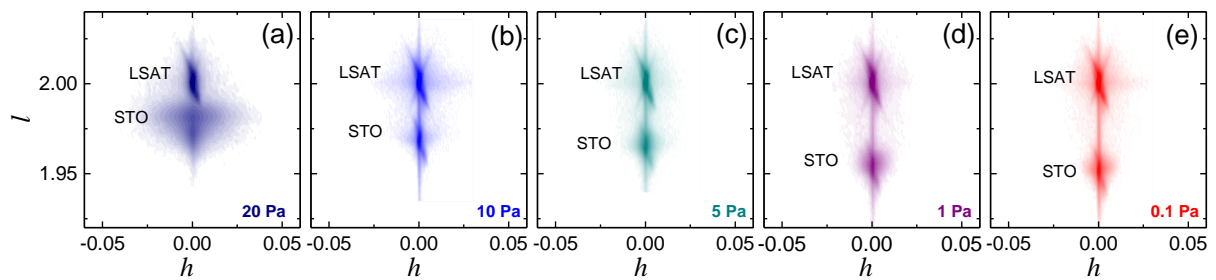


**Fig. S4.** Reciprocal space maps around (002) lattice points in the 150-nm-thick STO/LSAT films deposited at different pressures of oxygen. Coordinates are expressed in reciprocal lattice units of LSAT.

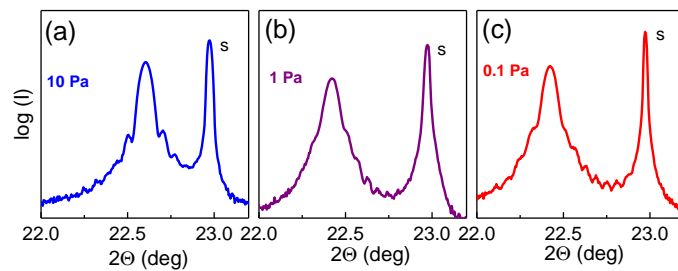


**Fig. S5.** Details of XRD  $\Theta$ - $2\Theta$  scans around (001) perovskite peaks in the 150-nm-thick STO films on LSAT. Deposition pressure is marked on the plots. Laue satellites evidence smooth films of high crystal quality.

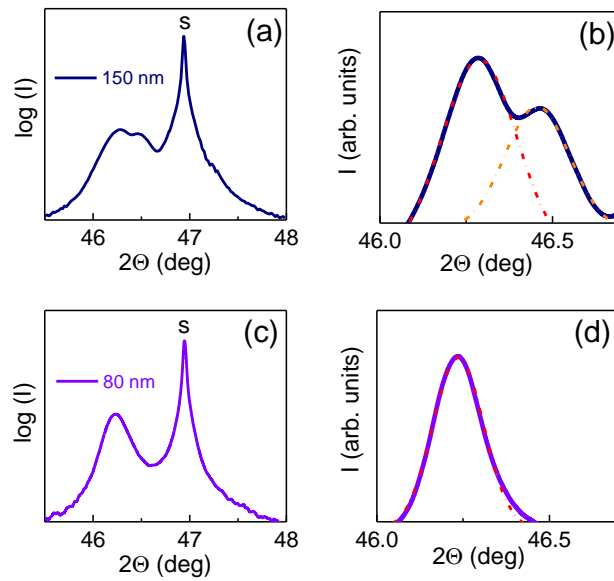


**Fig. S6.** XRD  $\Theta$ - $2\Theta$  scans around (002) perovskite peaks in the (a, b) 150-nm-thick and (c, d) 80-nm-thick STO films on LSAT. Deposition pressure is 20 Pa. Strain relaxation is evidenced by the two phases – strained and relaxed – in the 150-nm-thick film.

#### S4. Optical losses

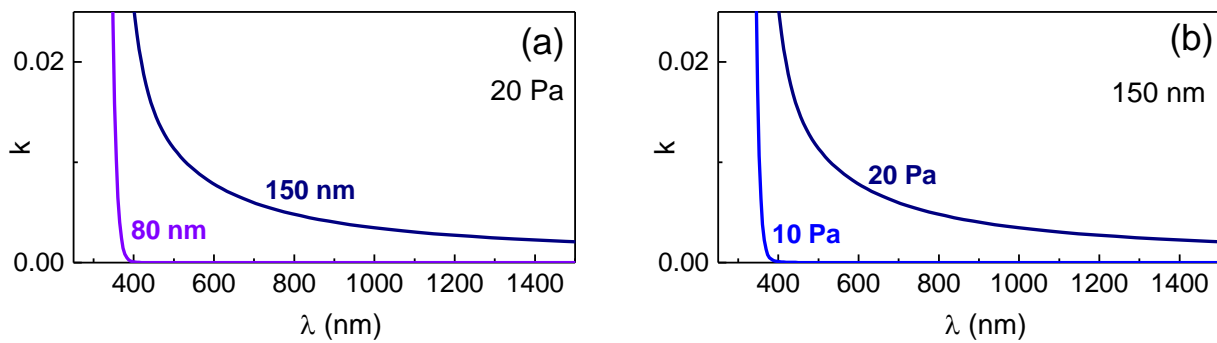


**Fig. S7.** Extinction coefficient as a function of wavelength in the (a) films of different thicknesses deposited at 20 Pa and (b) films of 150 nm in thickness deposited at different pressures.

### S5. Anisotropic chemical expansion.

The unit cell of a material, from which the film is made, is assumed to be tetragonal with the lattice parameters ( $a_0$ ,  $c_0$ ), tetragonality ( $t_0$ ), and unit-cell volume ( $V_0$ ):

$$c_0 = t_0 a_0 \quad (7)$$

$$V_0 = t_0 a_0^3 = V_{STO} = (3.905 \text{Å})^3 \quad (8)$$

The unit-cell volume in the film is  $V$ :

$$V = ca^2 = t_0 a_0^3 (1 + s_a)^2 \left(1 - \frac{2c_{12}}{c_{11}} s_a\right) \quad (9)$$

$$\frac{V}{V_0} = (1 + s_a)^2 \left(1 - \frac{2c_{12}}{c_{11}} s_a\right) \quad (10)$$

Or in another form:

$$\left(\frac{V}{V_{STO}} - 1\right) = \left(2 - \frac{2c_{12}}{c_{11}}\right) s_a + \left(1 - \frac{4c_{12}}{c_{11}}\right) s_a^2 - \frac{2c_{12}}{c_{11}} s_a^3 \quad (11)$$

Here, equation (11) was solved graphically for the strain  $s_a$  using the measured unit-cell volume of the films ( $V$ ). Then the tetragonality of the material was calculated for each film:

$$t_0 = \frac{c(1+s_a)}{a\left(1 - \frac{2c_{12}}{c_{11}} s_a\right)} \quad (12)$$

### S6. Tetragonal material.

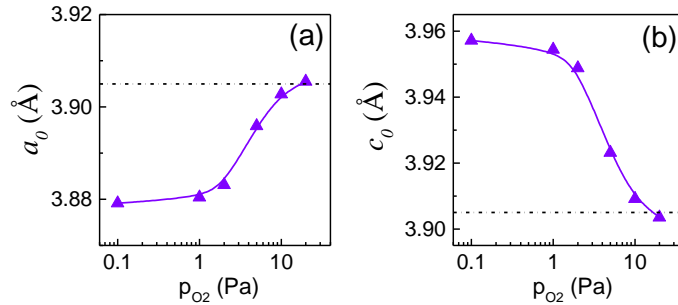


**Fig. S8.** Lattice parameters of unstressed tetragonal material estimated from the measured parameters of each of the films.

### S7. First-principles analysis of elastic properties.

To demonstrate high accuracy of *ab initio* calculations, the lattice parameters of misfit-strained stoichiometric STO and the elastic constants of STO were calculated. The in-plane strain  $\underline{s}_a = -0.95\%$ , corresponding to the STO/LSAT misfit strain, was considered. The in-plane lattice parameters of the model cubic STO were reduced, respectively, and the out-of-plane parameter was optimized. The optimization gave the out-of-plane strain  $s_c = 0.0057$ , tetragonality  $t = 1.015$ , and relative change of the unit-cell volume  $\Delta V = -1.33\%$ . These *ab initio* values are in excellent agreement with the theoretical macroscopic ones [see elastic relationships (1-6) above]. The calculated elastic constants  $c_{11} = 3.83 \times 10^{11} \text{ N/m}^2$  and  $c_{12} = 1.13 \times 10^{11} \text{ N/m}^2$  and the ratio  $c_{12}/c_{11} = 0.295$  practically coincide with the tabulated data. Here, minor overestimation of elastic constants occurs because the calculations are performed for the temperature  $T = 0 \text{ K}$  and the thermal expansion is consequently neglected.

### S8. Interaction of oxygen vacancy stress with misfit strain.

For an oxygen vacancy in the (001)[SrO] plane, the interaction energy of the vacancy stress (described by elastic dipole tensor)<sup>33</sup> with the STO/LSAT misfit strain is

$$E^{int}(eV) = - \begin{bmatrix} 4.53 & 0 & 0 \\ 0 & -2.1 & 0 \\ 0 & 0 & -2.1 \end{bmatrix} \times \begin{bmatrix} 0.0056 \\ -0.0095 \\ -0.0095 \end{bmatrix} \approx -0.065 \quad . \quad (13)$$

For an oxygen vacancy in the (001)[TiO] plane, the interaction energy with the STO/LSAT misfit strain is

$$E^{int}(eV) = - \begin{bmatrix} 4.53 & 0 & 0 \\ 0 & -2.1 & 0 \\ 0 & 0 & -2.1 \end{bmatrix} \times \begin{bmatrix} -0.0095 \\ -0.0095 \\ 0.0056 \end{bmatrix} \approx 0.035 \quad . \quad (14)$$

The density of elastic energy (energy per unit volume)  $W_s$ , which is associated with misfit strain  $s_a$ , can be calculated as

$$W_s = \frac{Y s_a^2}{(1-\nu)}, \quad (15)$$

where  $Y$  and  $\nu$  are the Young's modulus and the Poisson's ratio, correspondingly.

We assume that the misfit elastic energy is fully compensated by the formation of non-interacting elastic dipoles caused by oxygen vacancies in the (001)[SrO] planes. Then the maximum concentration  $N$  of oxygen vacancy stress dipoles can be estimated as

$$N = \frac{Ys_a^2}{E^{int}(1-\nu)}. \quad (16)$$

For  $Y = 236$  GPa,  $\nu = 0.23$ ,  $s_a = -0.0095$ , and  $E^{int} = 0.065$  eV, we obtain  $N \approx 2 \times 10^{27} \text{ m}^{-3}$ , which is nearly two orders of magnitude smaller than the concentration of atoms in STO. This estimation suggests that oxygen deficiency of less than 1 at % is sufficient for stabilizing epitaxial growth and raising the critical thickness in the STO/LSAT films.

### S9. Residual strain.

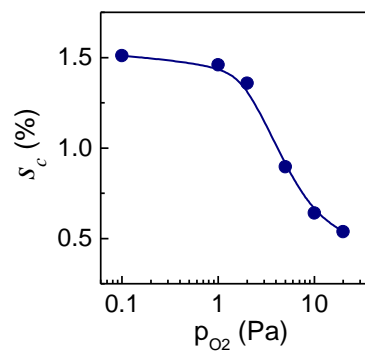


**Fig. S9.** Out-of-plane strain as a function of oxygen pressure in the 150-nm-thick STO/LSAT films.